Noise Behavior of Microwave Amplifiers Operating Under Nonlinear Conditions

Laurent Escotte, Eric Gonneau, Cédric Chambon, and Jacques Graffeuil, *Senior Member, IEEE*

***Abstract*—The noise behavior of microwave amplifiers operating under a large-signal condition has been studied in this paper. A Gaussian noise is added to a microwave signal and they are applied at the input of several amplifying devices. Experimental data show a decrease of the output noise spectral density when the power of the microwave signal at the input of the devices increases due to the compression of the amplifiers. A distortion component due to the interaction of the signal and its harmonics with the noise is also demonstrated from a simplified theoretical model. The statistical properties of the signal and the noise have also been investigated in order to verify the Gaussianity of the noise at the output of the nonlinear circuits. We have also observed that the majority of the measured devices show some variations of their additive noise versus the input power level.**

***Index Terms*—Microwave amplifiers, noise measurements, nonlinear device, signal and noise, spectral analysis.**

I. Introduction

THE mathematical theory of random signals and noise in nonlinear devices has been intensively investigated [1]–[7]. It was applied to the case of square-law detectors, half-wave linear detectors, or amplitude limiters. The effects of noise have been also studied in traveling-wave tube amplifiers [8] and in FM systems [9], [10]. Some of the studies concern only Gaussian noise at the input of the devices [5]–[7], while others rely on the addition of a signal and Gaussian noise [1]–[4]. In the latter, the particular case of a sine wave has also been studied.

However, all approaches remain theoretical and suffer from a lack of experimental data. A simple technique to characterize the noise figure (NF) of various silicon-based bipolar transistors has recently been proposed [11] when the devices are operated under nonlinear conditions. The results showed that the NF increases when the power at the input of the transistors increases and that the measured values are strongly correlated to the ones of the measured residual phase noise. The dependence of the NF on the input power of the signal has been also outlined in [12] and a new definition of the NF (noise and distortion figure) has been proposed by other authors [13]. The noise behavior of microwave amplifiers operating under nonlinear conditions must be accurately analyzed in order to evaluate the desensitization of RF receivers [14], [15]. This also becomes a critical point for each new generation of mobile phones [16] or in the case of multistandards systems. Indeed, some of the noise and signal at the output of the power amplifier can be coupled, through the duplexer, to the low-noise amplifier (LNA) input. The transmit signal, acting as an interferer, further increases the NF of the LNA, and this point needs careful investigations. There is also a special concern for assessing residual phase noise of microwave devices [11], [17] in order to design low-noise oscillators: in this case, the interaction of the input signal with noise is essential. Thus, we propose in this paper to investigate the noise properties of a few different microwave amplifiers operating under nonlinear conditions from both a theoretical and an experimental point-of-view.

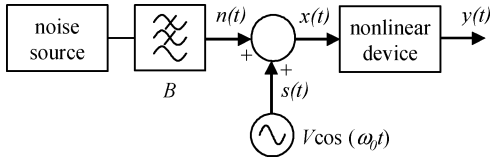

Fig. 1. Theoretical model used to calculate the power spectrum at the output of the nonlinear device.

Section II is then dedicated to the theoretical analysis and some general results are reported. The measurement technique proposed in [11] has been refined and is described in Section III. Moreover, time-domain measurements are reported in order to study the statistical properties of the signal and noise. The variations of the additive noise of the amplifiers versus the input power are analyzed with the help of frequency-domain measurements. Finally, Section IV presents the comparison between experimental data and theoretical results. The variations of the additive noise versus the input power of the amplifiers are then investigated.

II. Theoretical Analysis

The theoretical model of the investigated system is represented in Fig. 1. A white Gaussian noise delivered by a noise source passes through a low-pass filter (LPF) featuring an equivalent noise bandwidth B. The noise $n(t)$ featuring a constant power spectral density (PSD) $N/2$ over the bandwidth B is then added to the signal $s(t)$, which is assumed to be sinusoidal as follows:

$$s(t) = V\cos(\omega_0 t). \tag{1}$$

V and ω_0 represent the amplitude and angular frequency of the sine wave, respectively. The power spectrum of $x(t)$ at the input of the nonlinear device is given in Fig. 2.

Manuscript received February 3, 2005; revised April 29, 2005 and June 6, 2005.

L. Escotte, C. Chambon, and J. Graffeuil are with the Laboratoire d'Analyse et d'Architecture des Systèmes, Centre National de la Recherche Scientifique, 31077 Toulouse Cedex, France and also with the Electronic Engineering Department, Paul Sabatier Université, 31077 Toulouse Cedex, France (e-mail: escotte@laas.fr).

E. Gonneau is with the Laboratoire de Télédétection à Haute Résolution, Paul Sabatier Université, 31029 Toulouse Cedex, France (e-mail: gonneau@cict.fr).

Digital Object Identifier 10.1109/TMTT.2005.856082

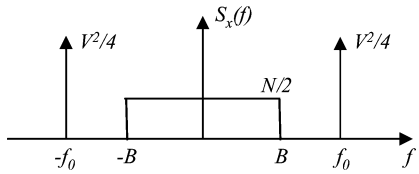

Fig. 2. Power spectrum of $x(t)$ at the input of the nonlinear device.

The frequency of the signal f_0 is arbitrarily chosen greater than the noise bandwidth in order to suit the experimental requirements. This can also correspond to the practical case where an interferer or a blocking signal is close, but outside the receiver bandwidth. The model given in Fig. 1 is close to the test set described in Section III-A where both the amplitude V of the signal and the input noise spectral density $N/2$ can be varied.

The problem is to determine the power spectrum $S_y(f)$ at the output of the device. For that purpose, the nonlinear circuit, supposed to be memoryless, is represented by the following expression:

$$y(t) = \sum_{i=1}^{n} \alpha_i x^i(t) \tag{2}$$

where α_i are the coefficients of the polynomial. This type of expression is generally used to describe nonlinearities even if it is well known that it cannot fully describe the complex nonlinear behavior of microwave amplifiers. The nonlinear device is assumed noiseless in a first step. The additive noise contributed by the noise sources located inside the two-port will be taken into account in Section IV. The theoretical analysis is then concentrated on the impact of an external noise entering a nonlinear device in the presence of a large sinusoidal signal. The degree n of the polynomial is fixed at 3 in order to reduce the length of the mathematical derivation, which is decomposed in two steps. In the first one, the autocorrelation function is calculated. The output spectrum is then expressed in the second step.

A. Autocorrelation Function

The autocorrelation function $R_y(\tau)$ of the output signal is calculated using the direct method [3]

$$R_y(\tau) = E\big[y(t)y(t+\tau)\big] \tag{3}$$

where $E[\,]$ is the expected value or the statistical average. Assuming $x(t) = x_1 = s_1 + n_1$ and $x(t+\tau) = x_2 = s_2 + n_2$, where subscripts 1 and 2 are related to the variables t and $t+\tau$, respectively, (3) can be rewritten as

$$\begin{aligned} R_y(\tau) &= E\big[x_1x_2\big(\alpha_1 + \alpha_2x_1 + \alpha_3x_1^2\big)\big(\alpha_1 + \alpha_2x_2 + \alpha_3x_2^2\big)\big] \\ &= \alpha_1^2E\big[x_1x_2\big] + \alpha_2^2E\big[x_1^2x_2^2\big] + \alpha_3^2E\big[x_1^3x_2^3\big] \\ &\quad + 2\alpha_1\alpha_2E\big[x_1x_2^2\big] + 2\alpha_1\alpha_3E\big[x_1x_2^3\big] \\ &\quad + 2\alpha_2\alpha_3E\big[x_1^2x_2^3\big]. \end{aligned} \tag{4}$$

The autocorrelation function is then composed of six components, which are derived using the fact that the signal and noise are statistically independent and that the expected values of s_1, s_2, n_1, and n_2 are 0.

Furthermore, it can be easily found that, in the case of a sine wave and assuming ergodic process of the signal, $E[s_1^k s_2^l] = 0$ when the sum $k+l$ is an odd number. The same behavior can also be found for a Gaussian noise, as previously stated in [2] and [4], i.e., $E[n_1^k n_2^l] = 0$ when the sum $k+l$ is an odd number.

The components of $R_y(\tau)$ can then be expressed as

$$\begin{aligned} E\big[x_1x_2\big] &= E\big[s_1s_2\big] + E\big[n_1n_2\big] \\ &= R_s(\tau) + R_n(\tau) \end{aligned} \tag{5}$$

$$E\big[x_1x_2^2\big] = 0 \tag{6}$$

$$\begin{aligned} E\big[x_1^2x_2^2\big] &= E\big[s_1^2s_2^2\big] + E\big[s_1^2n_2^2\big] + E\big[n_1^2s_2^2\big] + E\big[n_1^2n_2^2\big] \\ &\quad + E\big[4s_1s_2n_1n_2\big] \\ &= R_{s^2}(\tau) + 2\sigma_s^2\sigma_n^2 + R_{n^2}(\tau) + 4R_s(\tau)R_n(\tau) \end{aligned} \tag{7}$$

$$\begin{aligned} E\big[x_1x_2^3\big] &= E\big[s_1s_2^3\big] + E\big[3s_1s_2n_2^2\big] + E\big[n_1n_2^3\big] + E\big[3s_2^2n_1n_2\big] \\ &= E\big[s_1s_2^3\big] + 3\sigma_n^2R_s(\tau) + E\big[n_1n_2^3\big] + 3\sigma_s^2R_n(\tau) \end{aligned} \tag{8}$$

$$E\big[x_1^2x_2^3\big] = 0 \tag{9}$$

$$\begin{aligned} E\big[x_1^3x_2^3\big] &= E\big[s_1^3s_2^3\big] + E\big[3s_1^3s_2n_2^2\big] + E\big[n_1^3n_2^3\big] \\ &\quad + E\big[3s_2^2n_1^3n_2\big] + E\big[3s_1s_2^3n_1^2\big] + E\big[9s_1s_2n_1^2n_2^2\big] \\ &\quad + E\big[3s_1^2n_1n_2^3\big] + E\big[9s_1^2s_2^2n_1n_2\big] \\ &= R_{s^3}(\tau) + 6\sigma_n^2E\big[s_1^3s_2\big] + R_{n^3}(\tau) + 6\sigma_s^2E\big[n_1^3n_2\big] \\ &\quad + 9R_s(\tau)R_{n^2}(\tau) + 9R_{s^2}(\tau)R_n(\tau) \end{aligned} \tag{10}$$

where $\sigma_s^2 = E[s_1^2] = E[s_2^2] = R_s(0)$ corresponds to the variance of the signal and $\sigma_n^2 = E[n_1^2] = E[n_2^2] = R_n(0)$ corresponds to the variance of the noise.

Concerning the signal, the following equations can be easily obtained:

$$R_{s^2}(\tau) = 0.5\sigma_s^4 + R_s^2(\tau) \tag{11}$$

$$R_{s^3}(\tau) = 1.5\sigma_s^4R_s(\tau) + R_s^3(\tau) \tag{12}$$

$$E\big[s_1s_2^3\big] = 1.5\sigma_s^2R_s(\tau). \tag{13}$$

Concerning the noise, and using Price's theorem [6], the following equations can be derived, which are in agreement with [7]:

$$R_{n^2}(\tau) = \sigma_n^4 + 2R_n^2(\tau) \tag{14}$$

$$R_{n^3}(\tau) = 9\sigma_n^4R_n(\tau) + 6R_n^3(\tau) \tag{15}$$

$$E\big[n_1n_2^3\big] = 3\sigma_n^2R_n(\tau). \tag{16}$$

Equations (11)–(16) are injected into (5)–(10) and the new expressions are then used to calculate the expression of the autocorrelation function of the output signal $y(t)$

$$\begin{aligned} R_y(\tau) &= \alpha_2^2\big(0.5\sigma_s^4 + 2\sigma_s^2\sigma_n^2 + \sigma_n^4\big) + K_sR_s(\tau) + \alpha_2^2R_s^2(\tau) \\ &\quad + \alpha_3^2R_s^3(\tau) + K_nR_n(\tau) + 2\alpha_2^2R_n^2(\tau) \\ &\quad + 6\alpha_3^2R_n^3(\tau) + 4\alpha_2^2R_s(\tau)R_n(\tau) \\ &\quad + 18\alpha_3^2R_s(\tau)R_n^2(\tau) + 9\alpha_3^2R_s^2(\tau)R_n(\tau) \end{aligned} \tag{17}$$

where the coefficients K_s and K_n are as follows:

$$K_s = \big(\alpha_1 + 3\alpha_3\sigma_n^2\big)^2 + 3\sigma_s^2\Big(\alpha_1\alpha_3 + \alpha_3^2\big(0.5\sigma_s^2 + 3\sigma_n^2\big)\Big) \tag{18}$$

$$K_n = \big(\alpha_1 + 3\alpha_3\sigma_n^2\big)^2 + 6\sigma_s^2\Big(\alpha_1\alpha_3 + \alpha_3^2\big(0.75\sigma_s^2 + 3\sigma_n^2\big)\Big). \tag{19}$$

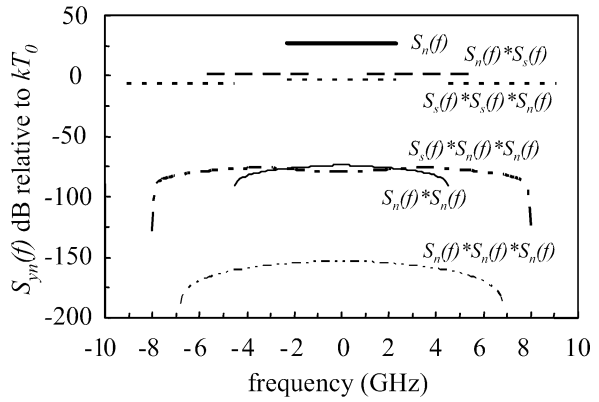

Fig. 3. Output noise spectral density $S_{yn}(f)$ showing the different components. The dc component and the spectrum related to the signal are not plotted. $f_0 = 3.4$ GHz, $V = 25$ mV, $B = 2.3$ GHz, and $N = kT_0$ with $T_0 = 290$ K, $\alpha_1 = 33.5$, $\alpha_2 = 70$, and $\alpha_3 = -1450$.

B. Output Spectrum

The PSD of the output signal is obtained by taking the Fourier transform of the autocorrelation function given by (17)

$$\begin{aligned} S_y(f) = {} & \alpha_2^2\left(0.5\sigma_s^4 + 2\sigma_s^2\sigma_n^2 + \sigma_n^4\right)\delta(f) + K_s S_s(f) \\ & + \alpha_2^2 S_s(f) * S_s(f) + \alpha_3^2 S_s(f) * S_s(f) * S_s(f) \\ & + K_n S_n(f) + 2\alpha_2^2 S_n(f) * S_n(f) \\ & + 6\alpha_3^2 S_n(f) * S_n(f) * S_n(f) \\ & + 4\alpha_2^2 S_s(f) * S_n(f) \\ & + 9\alpha_3^2 S_s(f) * S_s(f) * S_n(f) \\ & + 18\alpha_3^2 S_s(f) * S_n(f) * S_n(f). \end{aligned} \quad (20)$$

$\delta(f)$ represents the Dirac–delta function and the symbol $*$ denotes the convolution product.

The output spectrum can be decomposed in several components [3], [18]. The first term in the first line in (20) corresponds to the dc component ($S_y(0)$). The last term in the first line and the second line correspond to the interaction of the signal with itself ($S_{ysxs}(f)$). Lines 3 and 4 correspond to the interaction of the noise with itself ($S_{ynxn}(f)$). Lines 5–7 in (20) are related to the interaction of the signal with the noise ($S_{ysxn}(f)$). The different convolution products are given in the Appendix .

Fig. 3 represents the different components of the output noise spectral density ($S_{yn}(f) = S_{ynxn}(f) + S_{ysxn}(f)$) calculated from (20) and from the different expressions given in the Appendix . The amplitude of the signal is fixed at 25 mV corresponding to an input power of -22 dBm ($Z_c = 50\,\Omega$). The value of f_0 is set to 3.4 GHz and is greater than the noise bandwidth B, which is equal to 2.3 GHz. The input noise power density is given by $N = kT_0$, assuming that T_0 corresponds to the standard temperature (290 K) and k is the Boltzmann's constant. The coefficients α_i are those of amplifier #1 described in Section III. All the components appearing in Fig. 3 are normalized with respect to kT_0. It can be seen that the interaction of the signal with noise impacts in many different bandwidths and that the noise level rises as the input power increases. The different components $S_n(f)$, $S_n(f) * S_s(f)$, and $S_s(f) * S_s(f) * S_n(f)$ are overlapping between the frequencies $f_0 - B$ and B corresponding to 1.1 and 2.3 GHz, respectively.

It can be shown that several components can be neglected in the output noise spectrum. The components $S_n(f) * S_n(f)$ and $S_n(f) * S_n(f) * S_s(f)$ are 100 dB lower than the value corresponding to $S_n(f)$ in the noise bandwidth, while the $S_n(f) * S_n(f) * S_n(f)$ component is found to be even more negligible. This is mainly due to the fact that N^2 and N^3 are much lower than N. It can also be noted that the variance of the noise σ_n^2, which is equal to BN, is also negligible when comparing its value to the variance of the signal $\sigma_s^2 = V^2/2$. This simplifies the expressions of K_s and K_n given by (18) and (19). Therefore, if we concentrate on the noise PSD at the output, $S_{yn}(f)$ can be approximately given as

$$\begin{aligned} S_{yn}(f) = {} & K_n S_n(f) + 4\alpha_2^2 S_s(f) * S_n(f) \\ & + 9\alpha_3^2 S_s(f) * S_s(f) * S_n(f). \end{aligned} \quad (21)$$

III. Frequency- and Time-Domain Experimental Setup, Characteristics of Investigated Devices, Time-Domain Results

Firstly, the frequency-domain experimental setup and procedure is described and some essential characteristics of the amplifiers that will be later measured are given. Secondly, the test-set modifications needed for time-domain measurements are presented in order to check the assumption of Gaussianity of the noise at the output of the different devices.

A. Frequency-Domain Measurements

The experimental setup used to characterize the different amplifiers in the frequency domain is reported in Fig. 4. Some differences from the one previously described in [11] have been introduced.

A spectrum analyzer is now used to measure the different harmonics level at the output of the amplifier. This allows to evaluate the output power at 1-dB compression gain ($P_{s1\,\mathrm{dB}}$) and to calculate the total harmonic distortion (THD) at the output of the device-under-test (DUT). The maximum power delivered by the RF synthesizer at f_0 is adjusted for each amplifier in order to obtain the same nonlinear condition fixed at 3-dB compression gain. In this case, the THD calculated up to the third harmonic is close to the one calculated using five harmonics since the deviation is less than 0.7% for all the investigated amplifiers.

The LPFs were characterized using a network analyzer in order to determine their transfer function. The S_{21}-parameter of the LPFs exhibits a minimum value (-60 dB) at a frequency of 3.4 GHz, which has been chosen for f_0. The power gain is then modeled (up to f_0) using the Butterworth function, and the equivalent noise bandwidth is calculated using the conventional equation [19]. The value of B is equal to 2.3 GHz. The LPF located after the noise source is used in order to match the experimental test set to the theoretical model reported in Fig. 1. The same experiment has also been carried out using a narrow-band filter centered at the same frequency where the noise is measured: results are essentially unchanged and will not be addressed further.

The LPF located in the receiver (represented in the dashed box in Fig. 4) is used to attenuate the RF signal at f_0, ensuring a linear behavior of the noise receiver. The noise is measured

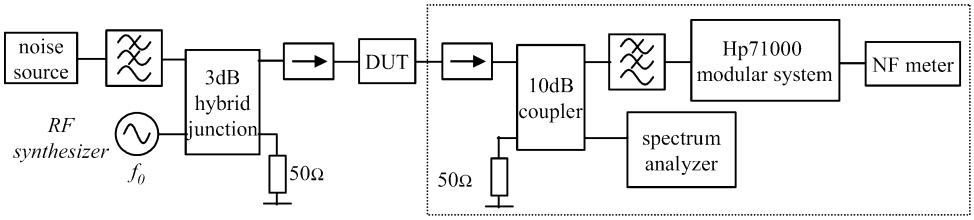

Fig. 4. Experimental setup used to determine the noise PSD at the output of the amplifier operating under nonlinear condition.

at a lower frequency (2 GHz), which is compatible with the different frequency bands of the various microwave elements used in the setup. This measurement principle is identical to the one described in [11] and is also used to characterize the hot small-signal S-parameters of microwave power transistors [20]. The DUT is located between two isolators in order to reduce mismatch uncertainties when measuring the noise powers [21]. The noise and RF signal are combined at the input of the DUT with the help of a 3-dB hybrid junction. The losses of the two-port, including the LPF, the 3-dB coupler, and the input isolator, are measured at 2 GHz for appropriate correction in the NF meter. The same thing is also performed for the two-port located between the RF synthesizer and the isolator output at $f_0 = 3.4$ GHz in order to precisely know the power at the input of the DUT. The noise receiver is calibrated when the RF signal is *off* and without the DUT. The NF meter measures the noise power at an intermediate frequency of 22 MHz [11] when the noise source is alternatively *off* and *on* and the corrected noise power spectral densities relative to kT_0 are then displayed. The characteristics of the measured amplifiers at 2 GHz are reported in Table I. The gain and NF are measured under small-signal conditions (without RF signal). All these devices are commercially available amplifiers and detailed information about their internal configurations is not available.

TABLE I
CHARACTERISTICS OF THE MEASURED AMPLIFIERS AT 2 GHz

Amplifier	Bandwidth (GHz)	Gain (dB)	NF (dB)	P_{s1dB} (dBm)	THD (%)[a]
#1	2-22	30.5	2.05	15.5	29.1
#2	1-4	33	1	11	19.3
#3	2-8	39	2.9	18	28.3
#4	0.01-2	23	5.2	17	6.4

[a] the THD is calculated using 5 harmonics, at 3 dB compression gain

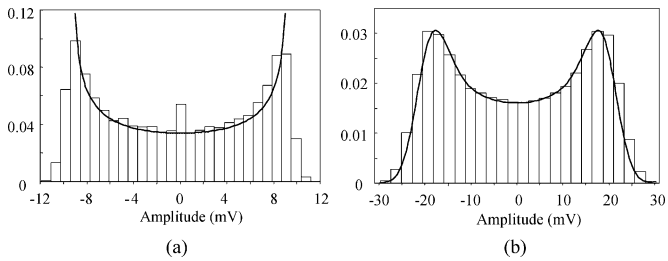

Fig. 5. PDFs. (a) Sinusoidal signal. (b) Sinusoidal and Gaussian noise. Solid lines correspond to theoretical expressions.

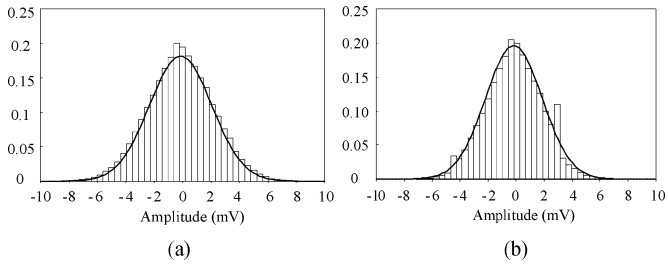

Fig. 6. PDFs of the noise at the output of amplifier #1. (a) Linear conditions. (b) Nonlinear conditions.

B. Time-Domain Measurements

Time-domain measurements are performed with the help of a 6-GHz bandwidth digital oscilloscope that has been substituted for the NF meter and spectrum analyzer of Fig. 4 at the DUT output. The statistical properties of the signal and the noise at the output of the DUT can then be investigated. Two basic experiments are first performed.

The first of these consists of measuring the signal delivered by the RF synthesizer and of calculating its probability density function (PDF). In the second experiment, we determine the PDF of the signal plus the noise combined within a 3-dB hybrid junction. The noise source is *on* and is amplified using a broad-band LNA (10 kHz–1 GHz) in order to be larger than the noise level of the oscilloscope. The results are reported in Fig. 5(a) and (b). 800 000 points are used in the statistical analysis and the width of the classes in the different histograms is limited by the sensibility of the oscilloscope.

The PDF of the sinusoidal signal reported in Fig. 5(a) is in agreement with the expected result [19] reported as follows:

$$f_s(x) = \frac{1}{\pi V} \frac{1}{\sqrt{1 - \left(\frac{x}{V}\right)^2}}. \tag{22}$$

The maximum value (V) of the voltage is approximately 10 mV and the calculated value of the density function at 0 V corresponds to $1/(\pi V)$. The PDF of the signal plus the noise is plotted in Fig. 5(b). The theoretical plot corresponds to the convolution of the PDF of the signal with the PDF of the Gaussian noise [22]. The amplitude of the signal is 20 mV and the standard deviation of the noise is 3 mV. Here, again, a good agreement is observed between theoretical and measured data.

In a second step, we aim at investigating the behavior of the noise at the output of a microwave amplifier. Two cascaded LPFs located after the DUT are used to ensure a better attenuation of the tone at f_0 and at the different harmonics. They are needed in order to estimate the PDF of the output noise only. If these filters were not present, the PDF would be modified by the tone and this would lead to a PDF similar to the one of Fig. 5(b). The results corresponding to amplifier #1 are reported in Fig. 6(a) and (b) when the RF signal is *off* and *on*, respectively. In the latter,

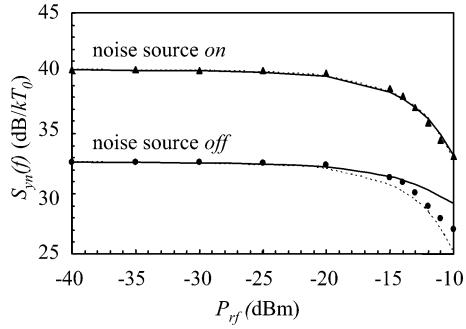

Fig. 7. Output noise spectral density $S_{yn}(f)$ of amplifier #1 versus input power $P_{\rm rf}$ at $f = 2$ GHz. Symbols: measured data. Solid lines: $T_{\rm out}$ is constant. Dashed lines: $T_{\rm in}$ is constant.

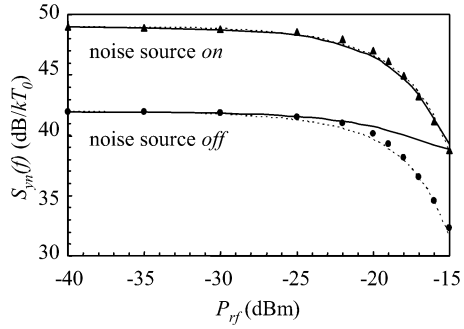

Fig. 9. Output noise spectral density $S_{yn}(f)$ of amplifier #3 versus input power $P_{\rm rf}$ at $f = 2$ GHz. Symbols: measured data. Solid lines: $T_{\rm out}$ is constant. Dashed lines: $T_{\rm in}$ is constant.

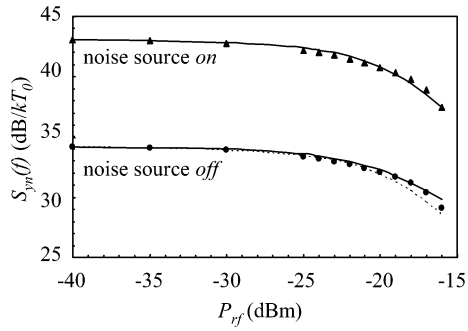

Fig. 8. Output noise spectral density $S_{yn}(f)$ of amplifier #2 versus input power $P_{\rm rf}$ at $f = 2$ GHz. Symbols: measured data. Solid lines: $T_{\rm out}$ is constant. Dashed lines: $T_{\rm in}$ is constant.

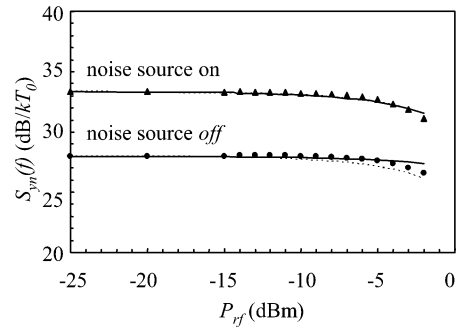

Fig. 10. Output noise spectral density $S_{yn}(f)$ of amplifier #4 versus input power $P_{\rm rf}$ at $f = 2$ GHz. Symbols: measured data. Solid lines: $T_{\rm out}$ is constant. Dashed lines: $T_{\rm in}$ is constant.

the input power is -10 dBm corresponding to 3-dB compression gain. The density function of the noise at the output of the amplifier without any RF signal [see Fig. 6(a)] closely fits the normal law, which validates the assumption of a Gaussian noise in the mathematical model of Section II. This result is also confirmed when calculating the higher order moments (μ_3 and μ_4) of the distribution in order to check the Gaussianity of the noise.

The PDF of the noise at the output of the amplifier operating under a nonlinear condition is reported in Fig. 6(b) and is again compared to the normal law. A good agreement is still observed and a deviation less than 7% is obtained between the theoretical value and the measured one of the fourth-order moment μ_4. It can, therefore, be stated that the statistical properties of a noise passing through a nonlinear device remain unchanged. This statement is experimentally verified as long as an efficient filtering of the tone pumping the nonlinear device is provided.

IV. Results and Discussion

The experimental results are reported in Figs. 7–10 for the different amplifiers. The noise power spectral densities relative to kT_0 are plotted versus the power at the input of the DUT ($P_{\rm rf}$). The measurements are performed when the noise source is *off* and *on*, corresponding to a noise temperature at the input of the devices equal to 297 K (T_c) and 2625 K (T_h), respectively. All the amplifiers exhibit the same behavior. The noise PSD decreases when $P_{\rm rf}$ increases. For example, we observe in Fig. 7, a deviation of 7 dB between the small-signal value of the noise PSD and the value measured (when the noise source is *on*) at $P_{\rm rf} = -10$ dBm, corresponding to the case of 3-dB compression gain for device #1. It can then be concluded that the behavior of the signal and the noise are very different, as previously stated in [23]. This observation is valid for devices #1–#3. Amplifier #4 exhibits different microwave performances than the other amplifiers (small gain and high NF), but the harmonic distortion is very low.

The variations of the noise PSD versus $P_{\rm rf}$, reported in Fig. 10, are small compared to the other amplifiers and a deviation of approximately 2.5 dB is observed when the noise source is *on*. This indicates that the noise behavior of the devices operating under nonlinear conditions is closely correlated to the harmonics level. The experimental results are compared to the theoretical model. The noise PSD is given from (21) where the values of $S_{ns}(f)$ and $S_{ns^2}(f)$, given in the Appendix, are calculated in the case where f_0 is greater than B. The expression of $S_{yn}(f)$ is then obtained assuming a single-sided band spectrum for a better comparison with experimental data as follows:

$$S_{yn}(f)=\left(\alpha_1^2+3\alpha_1\alpha_3V^2+\frac{9}{8}\alpha_3^2V^4\right)N+\alpha_2^2V^2N+\frac{9}{8}\alpha_3^2V^4N. \tag{23}$$

This equation indicates that the noise PSD at the output of the nonlinear device is the sum of three components. The first one is the consequence of the amplification of the input noise. It decreases as the input power increases ($\alpha_3 < 0$) due to gain

compression. The second component is related to the interaction, or the mixing, of the noise with the fundamental frequency of the signal. The last component corresponds to the interaction of the noise with harmonic 2 of the signal. This last component becomes higher than the other ones when the device is strongly nonlinear.

A fraction of the measured output noise is also contributed by the noise generated inside the device itself, which we call additive noise. Its PSD (N_a) is added to (23) in order to give the final expression of the output noise PSD, which is compared to experimental data

$$S_{yn}(f) = H_n N + N_a \tag{24}$$

where H_n is given by

$$H_n = \alpha_1^2 + \left(3\alpha_1\alpha_3 + \alpha_2^2\right)V^2 + \frac{9}{4}\alpha_3^2 V^4. \tag{25}$$

The values of N correspond to kT_c and kT_h when the noise source is *off* and *on*, respectively. The main problem is to determine the value of the additive noise. A simple solution consists of determining the value of N_a (N_a can be written as $kT_{\rm out}$, where $T_{\rm out}$ is the noise temperature at the output of the amplifier) without any RF signal (or under small-signal condition) and of considering this value as independent of $P_{\rm rf}$. This assumption has been used by other authors [13], [23], but it is not realistic since the noise is distributed differently along the different active devices from the input to the output of the amplifier.

However, two limiting cases can be evaluated. The first one consists of assuming $T_{\rm out}$ as a constant (the noise is located at the output of the amplifier). It corresponds to the solid lines in Figs. 7–10. In the other case (dashed lines), the noise source is located at the input of the amplifier (input noise temperature $T_{\rm in}$ supposed to be constant) and the additive noise is given by $H_n kT_{\rm in}$.

Two sets of coefficients α_i ($T_{\rm in}$ = constant and $T_{\rm out}$ = constant) can then be extracted for each amplifier. α_1 is determined under small-signal condition and the coefficients α_2 and α_3 are adjusted using a least square function in order to fit the measured values of $S_{yn}(f)$ when the noise source is *on*. In that case, the additive noise (N_a) is lower than the noise at the output of the device due to the amplified noise source ($H_n kT_h$). This is particularly verified for amplifier #2 featuring a low NF. For this example reported in Fig. 8, the additive noise is negligible (noise source *on*) and only one set of coefficients is found. A constant value of $T_{\rm out}$ seems to be a good approximation for this amplifier, but it is not the case for the other devices. As reported in Fig. 9, amplifier #3 exhibits the opposite behavior since a constant value of $T_{\rm in}$ seems to be a valuable assumption in order to fit the variations of $S_{yn}(f)$ versus $P_{\rm rf}$ when the noise source is *on* and *off*. Amplifiers #1 and #4 show a dependence of $T_{\rm in}$ or $T_{\rm out}$ on the input power $P_{\rm rf}$. This is also certainly the case for amplifier #2 for $P_{\rm rf}$ higher than -13 dBm. Our experimental results show that the noise behavior and particularly the additive noise of the microwave amplifiers operating under nonlinear conditions vary from one device to another. The observed variations of $T_{\rm in}$ or $T_{\rm out}$ versus $P_{\rm rf}$ are certainly due to the distributed nature of the noise sources and the nonlinearities inside the amplifiers.

V. Conclusion

The impact of input noise on small-signal microwave amplifiers operating under nonlinear conditions has been presented in this paper. It is the first time, to our knowledge, that experimental results have been reported on this topic.

We have compared the measured values of the output noise PSD with those given by a model based on the mathematical analysis of a sinusoidal signal and a Gaussian noise simultaneously passing through a nonlinear device. A polynomial model of the nonlinear amplifier transfer function has been demonstrated to be efficient in order to predict the interaction of the noise with the signal and its harmonics.

The statistical properties of the noise have also been studied showing that it remains Gaussian at the output of the amplifiers driven into large-signal condition. It has further been found that the additive noise depends on the input power. This behavior could be attributed to the distributed nature of both the noise sources and nonlinearities among the different devices of the multistages amplifiers.

This last point could be verified in a future study by measuring, for example, cascaded amplifiers with small gain or by using "homemade" amplifiers where nonlinear models of active devices are available.

Appendix

A. Convolution Products of the Signal

Assuming a sinusoidal signal, the different PSDs are reported as follows:

$$\begin{aligned} S_s(f) &= 0.5\sigma_s^2\left[\delta(f-f_0)+\delta(f+f_0)\right] \\ S_s(f) * S_s(f) &= 0.5\sigma_s^4\delta(f) \\ &\quad +0.25\sigma_s^4\left[\delta(f-2f_0)+\delta(f+2f_0)\right] \\ S_s(f) * S_s(f) * S_s(f) &= 0.375\sigma_s^6\left[\delta(f-f_0)+\delta(f+f_0)\right] \\ &\quad +0.125\sigma_s^6\left[\delta(f-3f_0)+\delta(f+3f_0)\right]. \end{aligned}$$

B. Convolution Products of the Noise

The convolution between $S_n(f)$ and $S_n(f)$ is given by the following relation:

$$S_n(f) * S_n(f) = S_{n^2}(f) = \int_{-\infty}^{+\infty} S_n(u)S_n(f-u)du$$

where u is a temporary variable needed for performing the integration. Assuming that $S_n(f)$ has the shape given in Fig. 2, the following equations can be derived:

$$\begin{aligned} &S_{n^2}(f) = \frac{N^2}{4}\left(2B - |f|\right), \qquad \text{for } -2B \le f \le 2B \\ &S_{n^2}(f) = 0, \qquad \text{for other frequencies.} \end{aligned}$$

The component $S_n(f) * S_n(f) * S_n(f)$ is noted $S_{n^3}(f)$ and is given by the following equations:

$$S_{n^3}(f) = \int_{-\infty}^{+\infty} S_{n^2}(u) S_n(f-u) du$$
$$S_{n^3}(f) = \frac{N^3}{16}(f+3B)^2, \quad \text{for } -3B \le f \le -B$$
$$S_{n^3}(f) = \frac{N^3}{8}(3B^2 - f^2), \quad \text{for } -B \le f \le B$$
$$S_{n^3}(f) = \frac{N^3}{16}(f-3B)^2, \quad \text{for } B \le f \le 3B$$
$$S_{n^3}(f) = 0, \quad \text{for other frequencies.}$$

C. Convolution Products of the Signal by the Noise

The convolution product between $S_s(f)$ and $S_n(f)$ is noted $S_{ns}(f)$ and the following two cases must to be considered for calculating its expression.

For $f_0 > B$:

$$S_{ns}(f) = \sigma_s^2 \frac{N}{4}, \quad \text{for } -f_0 - B \le f \le -f_0 + B$$
$$\text{and for } f_0 - B \le f \le f_o + B$$
$$S_{ns}(f) = 0, \quad \text{for other frequencies.}$$

For $f_0 < B$:

$$S_{ns}(f) = \sigma_s^2 \frac{N}{4}, \quad \text{for } -f_0 - B \le f \le f_0 - B$$
$$\text{and for } B - f_0 \le f \le f_0 + B$$
$$S_{ns}(f) = \sigma_s^2 \frac{N}{2}, \quad \text{for } f_0 - B \le f \le B - f_0$$
$$S_{ns}(f) = 0, \quad \text{for other frequencies.}$$

The component $S_s(f) * S_s(f) * S_n(f)$ is noted $S_{ns^2}(f)$ and the following three cases are considered to derive its expression.

For $f_0 < B/2$:

$$S_{ns^2}(f) = \sigma_s^4 \frac{N}{8}, \quad \text{for } -2f_0 - B \le f \le -B$$
$$\text{and for } B \le f \le 2f_0 + B$$
$$S_{ns^2}(f) = \sigma_s^4 \frac{3N}{8}, \quad \text{for } -B \le f \le 2f_0 - B$$
$$\text{and for } -2f_0 + B \le f \le B$$
$$S_{ns^2}(f) = \sigma_s^4 \frac{N}{2}, \quad \text{for } 2f_0 - B \le f \le B - 2f_0$$
$$S_{ns^2}(f) = 0, \quad \text{for other frequencies.}$$

For $B/2 < f_0 < B$:

$$S_{ns^2}(f) = \sigma_s^4 \frac{N}{8}, \quad \text{for } -2f_0 - B \le f \le -B$$
$$\text{and for } B \le f \le 2f_0 + B$$
$$S_{ns^2}(f) = \sigma_s^4 \frac{3N}{8}, \quad \text{for } -B \le f \le -2f_0 + B$$
$$\text{and for } 2f_0 - B \le f \le B$$
$$S_{ns^2}(f) = \sigma_s^4 \frac{N}{4}, \quad \text{for } -2f_0 + B \le f \le 2f_0 - B$$
$$S_{ns^2}(f) = 0, \quad \text{for other frequencies.}$$

For $f_0 > B$:

$$S_{ns^2}(f) = \sigma_s^4 \frac{N}{8}, \quad \text{for } -2f_0 - B \le f \le -2f_0 + B$$
$$\text{and for } 2f_0 - B \le f \le 2f_0 + B$$
$$S_{ns^2}(f) = \sigma_s^4 \frac{N}{4}, \quad \text{for } -B \le f \le B$$
$$S_{ns^2}(f) = 0, \quad \text{for other frequencies.}$$

The component $S_n(f) * S_n(f) * S_s(f)$ is noted $S_{n^2s}(f)$ and the following two cases are considered to derive its expression.

For $f_0 > 2B$:

$$S_{n^2s}(f) = \frac{\sigma_s^2 N^2}{8}\big(2B - |f| + f_0\big),$$
$$\text{for } -f_0 - 2B \le f \le -f_0$$
$$\text{and for } f_0 \le f \le f_0 + 2B$$
$$S_{n^2s}(f) = \frac{\sigma_s^2 N^2}{8}\big(2B + |f| - f_0\big),$$
$$\text{for } -f_0 \le f \le -f_0 + 2B$$
$$\text{and for } f_0 - 2B \le f \le f_0$$
$$S_{n^2s}(f) = 0, \quad \text{for other frequencies.}$$

For $f_0 < 2B$:

$$S_{n^2s}(f) = \frac{\sigma_s^2 N^2}{8}\big(2B - |f| + f_0\big),$$
$$\text{for } -f_0 - 2B \le f \le -f_0$$
$$\text{and for } f_0 \le f \le f_0 + 2B$$
$$S_{n^2s}(f) = \frac{\sigma_s^2 N^2}{8}\big(2B + |f| - f_0\big),$$
$$\text{for } -f_0 \le f \le f_0 - 2B$$
$$\text{and for } -f_0 + 2B \le f \le f_0$$
$$S_{n^2s}(f) = \frac{\sigma_s^2 N^2}{4}\big(2B - f_0\big),$$
$$\text{for } f_0 - 2B \le f \le -f_0 + 2B$$
$$S_{n^2s}(f) = 0, \quad \text{for other frequencies.}$$

ACKNOWLEDGMENT

The authors thank Dr. N. Nolhier and Dr. E. Tournier, both of the Laboratoire d'Analyse et d'Architecture des Systèmes, Centre National de la Recherche Scientifique (LAAS–CNRS), Toulouse, France, for their help during amplifier measurements and mathematical derivation, respectively.

REFERENCES

[1] S. O. Rice, "Mathematical analysis of random noise," *Bell Syst. Tech. J.*, vol. 24, pp. 46–156, 1945.

[2] D. Middleton, "Some general results in the theory of noise through nonlinear devices," *Quart. Appl. Math.*, vol. 5, pp. 445–498, 1948.

[3] W. B. Davenport, Jr. and W. L. Root, *An Introduction to the Theory of Random Signals and Noise*. New York: IEEE Press, 1987, pp. 250–276.

[4] H. B. Shutterly, "General results in the mathematical theory of random signals and noise in nonlinear devices," *IEEE Trans. Inf. Theory*, vol. IT-9, no. 4, pp. 74–84, Apr. 1963.

[5] R. F. Baum, "The correlation function of smoothly limited Gaussian noise," *IRE Trans. Inf. Theory*, vol. IT-3, no. 9, pp. 193–197, Sep. 1957.

[6] R. Price, "A useful theorem for nonlinear devices having Gaussian inputs," *IRE Trans. Inf. Theory*, vol. IT-4, no. 6, pp. 69–72, Jun. 1958.

[7] R. F. Baum, "The correlation function of Gaussian noise passed through nonlinear devices," *IEEE Trans. Inf. Theory*, vol. IT-15, no. 7, pp. 448–456, Jul. 1969.
[8] O. Shimbo, "Effects of intermodulation, AM–PM conversion, and additive noise in multicarrier TWT systems," *Proc. IEEE*, vol. 59, no. 2, pp. 230–238, Feb. 1971.
[9] M. L. Liou, "Noise in an FM system due to an imperfect linear transducer," *Bell Syst. Tech. J.*, pp. 1537–1561, Nov. 1966.
[10] T. G. Cross, "Intermodulation noise in FM systems due to transmission deviations and AM/PM conversion," *Bell Syst. Tech. J.*, pp. 1749–1773, Dec. 1966.
[11] G. Cibiel, L. Escotte, and O. Llopis, "A study of the correlation between high-frequency noise and phase noise in low-noise silicon-based transistors," *IEEE Trans. Microw. Theory Tech.*, vol. 52, no. 1, pp. 183–189, Jan. 2004.
[12] S. L. Delage and J. Obregon, "Comments on noise source modeling for cyclostationary noise analysis in large-signal device operation," *IEEE Trans. Electron Devices*, vol. 50, no. 10, p. 2183, Oct. 2003.
[13] P. M. Lavrador, N. Borges de Carvalho, and J. C. Pedro, "Evaluation of signal-to-noise and distortion ratio degradation in nonlinear systems," *IEEE Trans. Microw. Theory Tech.*, vol. 52, no. 3, pp. 813–822, Mar. 2004.
[14] R. G. Meyer and A. K. Wong, "Blocking and desensitization in RF amplifiers," *IEEE J. Solid-State Circuits*, vol. 30, no. 8, pp. 944–946, Aug. 1995.
[15] A. Schneider and O. Werther, "Nonlinear analysis of noise in current-steering variable gain amplifiers," *IEEE J. Solid-State Circuits*, vol. 39, no. 2, pp. 290–296, Feb. 2004.
[16] T. Gee, "Suppressing errors in W-CDMA mobile devices," *Commun. Syst.*, vol. 7, no. 3, Mar. 2001. [Online].
[17] M. Rudolph and P. Heymann, "The influence of microwave two-port noise on residual phase noise in GaAs HBTs," in *Proc. 34th Eur. Microwave Conf.*, Amsterdam, The Netherlands, 2004, pp. 945–948.
[18] N. M. Blachman, "The signal x signal, noise x noise, and signal x noise output of a nonlinearity," *IEEE Trans. Inf. Theory*, vol. IT-14, no. 1, pp. 21–27, Jan. 1968.
[19] A. Ambrozy, *Electronic Noise*. New York: McGraw-Hill, 1982.
[20] T. Gasseling, D. Barataud, S. Mons, J. M. Nébus, J. P. Villotte, J. J. Obregon, and R. Quéré, "Hot small-signal S-parameter measurements of power transistors operating under large-signal conditions in a load–pull environment for the study of nonlinear parametric interactions," *IEEE Trans. Microw. Theory Tech.*, vol. 52, no. 3, pp. 805–812, Mar. 2004.
[21] "Noise figure measurement accuracy: The Y-factor method," Agilent Technol., Palo Alto, CA, Applicat. Note 57-2, 1976.
[22] L. J. Bain and M. Engelhardt, *Introduction to Probability and Mathematical Statistics*. Boston, MA: PWS-Kent, 1992.
[23] A. Geens and Y. Rolain, "Noise figure measurements on nonlinear devices," *IEEE Trans. Instrum. Meas.*, vol. 50, no. 4, pp. 971–975, Aug. 2001.

Laurent Escotte was born in Nouméa, France, in 1962. He received the Ph.D. degree in optic and microwave communications from the University of Limoges, Limoges, France, in 1988.

Since 1989, he has been an Assistant Professor of electronic engineering with the Paul Sabatier Université, Toulouse, France. At the same time, he joined the Laboratoire d'Analyse et d'Architecture des Systèmes du Centre National de la Recherche Scientifique (LAAS–CNRS), Toulouse, France. Since 1999, he has been a Professor of electronic engineering with the Paul Sabatier Université. His current research interests include noise characterization and modeling of active devices and circuits in the microwave and millimeter-wave frequency range. He has authored or coauthored over 50 technical papers and one book.

Eric Gonneau was born in Saint Pierre, Réunion Island, France, in 1965. He received the Ph.D. degree in signal processing from the Toulouse National Polytechnic Institute (INPT), Toulouse, France, in 1993.

Since 1994, he has been an Assistant Professor of electronic engineering with the Paul Sabatier Université, Toulouse, France. Until 2004, he was with the Laboratoire d'Acoustique de Métrologie et d'Instrumentation, where he specialized in sources localization using array processing and active noise reduction on multiple -input–output systems. Since 2005, he has been with the Laboratoire de Télédetection à Haute Résolution, where his current research interests are noise fluctuations, signal and multiresolution image processing. He has authored or coauthored over 30 technical papers.

Cédric Chambon was born in Limoges, France, on August 28, 1980. He received the M.S. degree in electronics from the University of Limoges, Limoges, France, in 2003, and is currently working toward the Ph.D. degree in electronics at the Laboratoire d'Analyse et d'Architecture des Systèmes du Centre National de la Recherche Scientifique (LAAS–CNRS), Toulouse, France.

His main field of interest is in the study of noise in microwave devices and circuits, more particularly, noise modeling and noise behavior in microwave amplifiers operating under nonlinear conditions, including the development of specific high-frequency noise measurement techniques.

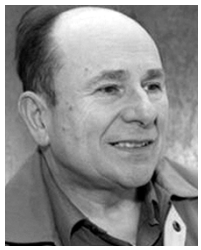

Jacques Graffeuil (SM'90) was born in Agen, France. He received the Ingénieur degree from the Institut National des Sciences Appliquées, Toulouse, France, in 1969, and the thèse d'Etat degree in electronic engineering from Paul Sabatier Université, Toulouse, France, in 1977.

Since 1970, he has been an Assistant Professor with Paul Sabatier Université. At that time, he joined the Laboratoire d'Analyse et d'Architecture des Systèmes, Centre National de la Recherche Scientifique (LAAS–CNRS), Toulouse, France, where he was engaged in research on noise in III–V semiconductor devices. He is currently a Professor of electronic engineering with Paul Sabatier Université and a Senior Scientist with the Microwave Devices and Integrated Circuits Group, LAAS–CNRS. His research initially dealt with Gunn effect devices and then with electrical properties of gallium–arsenide Schottky-barrier field-effect transistors (FETs). His current research involves noise and nonlinear properties of III–V FETs, HBTs and microwave silicon devices, silicon or III–V monolithic-microwave integrated-circuit (MMIC) design and microwave silicon microelectromechanical systems (MEMS). He has authored or coauthored over 150 technical papers and three books. He holds several patents.